Int. J. Electrochem. Sci., 16 **(2021)** Article ID: 210757, doi: 10.20964/2021.07.31

International Journal of ELECTROCHEMICAL SCIENCE
www.electrochemsci.org

Influence of N-Dodecyl Betaine Surfactant on Electroless Ni-P-nano-ZnO_2 Composite Coating Properties Prepared on Magnesium AZ91D Alloy

Manikandan Sundaraj[1,*], *Vijayakumar Subramani*[2]

[1] Department of Mechanical Engineering, University College of Engineering, Villupuram, Tamilnadu-605103, India.
[2] Department of Mechanical Engineering, University College of Engineering, Kancheepuram, Tamilnadu, India.
*E-mail: svmlmech@gmail.com

Received: 9 March 2021 / *Accepted:* 17 April 2021 / *Published:* 31 May 2021

Magnesium (AZ91D) alloy is used as structural components due to its high strength-to-weight ratio and high stiffness. A disadvantage of AZ91D is high surface roughness and poor corrosion resistance in the marine environment application. Therefore, for protection purposes, surface treatment or coating is required. Electroless plating was recognized for its excellent performance in recent years; its utilization rate has also increased dramatically over decades. This investigation carried in electroless Ni-P-nano-ZnO_2 composite coating on Mg AZ91D alloy with increasing activation by varying surfactant concentration N-dodecyl betaine (NDB). The coating is characterized by the scanning electron microscope and X-ray Analysis, surface hardness and, roughness measurement. Further, corrosion resistance of the coated substrate was identified using a neutral salt spray test. The results show that the optimal surfactant concentration of 0.6 g/l NDB improves corrosion resistance, reduces surface roughness, and improves surface hardness compared to coating without surfactant.

Keywords: Electroless coating, Nano Zinc Oxide, composite coating, Magnesium Alloy AZ91D, Neutral salt spray test, N-dodecyl betaine surfactant.

1. INTRODUCTION

Deposition nickel via autocatalytic or electroless deposition improves the corrosion resistance of the co-deposited particles. It is also found to enhance the mechanical, corrosion, and wear resistance properties on Substrates [1]. The most preferred method of composites coating is the electrochemical approach. In various industrial applications, electroless Ni-P composite coating is generally used with surfactant in the electrolyte, improving metallic electrons activation and reducing the wastage of nickel particles. Further, the surfactant dramatically enhances the mechanical properties and maintains the standard coating thickness on a substrate's surface [2].

The nanocomposite coating based on electroless plating has won great popularity in the preparations of the composite coating. Usually, adding nanoparticles to conventional electroless coating solution realizes the deposition of solid particles matrix [3]. The composite coating layer has higher corrosion resistance, wear resistance, better adhesion, and uniform coating. This process finds applications in aviation, electronics, machinery, and textiles [4].

Magnesium (Mg) AZ91D alloy has applications in structural components due to its very low density. It also finds applications in various mechanical applications where a high strength-to-weight ratio and high stiffness are essential [5]. Based on high specific strength and Young's modulus, the AZ91D shows better properties than Al and other lightweight metals[6]. It is weak to open environmental corrosion and poor wear resistance when the irregular deposition is formed on magnesium alloy's surface due to lack of metallic activation in the electrolyte [7]. The investigation on Ni-P-(sol) Al_2O_3 composite coating on Q235 steel with varying pH value shows an increase in hardness by adding Al_2O_3 in the Ni-P alloys coating structures by refining the grain. The pH value 4.5 of the electrolyte bath has the highest surface hardness value of about 569 HV. The hardness, friction factor, and corrosion resistance of the composite Al_2O_3 coating over Ni-P are higher than the NiP [8].

The addition of HND has avoided the micrometric defects of the sol-gel coating, and it also improved the corrosion resistance, and it is attributed to the film compactness, diffusion of the corrosive solution by tortuous pathways, and covering the defects by NHD [9].

In an electroless coating technique, the coating material to be deposited must be prepared as an electrolyte solution [10]. The electroless coating shows excellent corrosion resistance and good wear resistance [11]. However, so far, there is no much research on the use of surfactant in the electroless coating. Sometimes, the deposition would be successful, but the required amount of coating is not possible on the substrate and may resulting wastage of nickel due to insufficient electrons supplied to charged head [12]. It can be avoided or minimized by adding a surfactant to the electroless solution for improving electrochemical activation [13].

The surfactant can identify by the inclusion of formally charged groups in its head [14]. A non-ionic surfactant has no charge in its head [15]. The head of the ion surfactant will carry a charge [16]. The surfactant with a negative charge is anionic, and the positive is cationic [17]. Surfactant decreases the interfacial tension among the deposits, reduces the liquid solvent's surface tension, and improves the wetting and adsorption. It is leading to low porosity uniform thickness and increased thickness of coating in the substrate. The surfactant provides extra balance in opposition to air and moisture attack and easy handling [18].

The following surfactants are widely used in electroless coating. They are Sodium Dodecyl Sulfate (SDS) and cetyl trimethyl ammonium bromide (CTAB) surfactants [19] & [20]. Other surfactants such as Ammonium Lauryl Sulfate (ALS) [21], cationic-zwitterionic [22] have shown improvement in microhardness and surface roughness [23] & [24].

The surfactant's addition into the electrolyte solution will improve Ni particles' deposition and reduce the formation of H2 bubbles generated by the autocatalytic reaction, resulting in a coating with even deposition negligible porosity [25].

The adhesion properties are essential to form better bonding strength between the surface and substrate. Sometimes, deposits exhibit such kinds of problems as radial micro-cracks and delamination entire on the surface of the substrate [26], [27] & [28]. The N-dodecyl betaine (NDB) surfactant helps decrease the electrolyte's surface tension by forming micelles in the electrolyte to form better surface adhesion properties on the substrate [29].

The surfactants influence the process parameters, such as electrochemical bath, temperature, and pH of the electrolyte and deposition rate [16]. The correct proportion of electrochemical solutions may produce better surface properties like smooth coating surface, uniform coating thickness, and better mechanical properties. The maintenance of the optimal quantity of surfactant in the electrolyte bath will reduce surface tension, which improves the uniform dispersion of nanoparticles in the composite coating over the substrate [30]. The higher weight percentage of nanoparticles in the composite layer exhibits good mechanical properties [31]&[32].

The literature survey shows that the detailed analysis of the Ni-P-nano ZnO_2 composite coating on the Mg AZ91D with NDB surfactant is not reported. This work attempts to investigate the effect of volume fraction of NDB surfactant on the electrolyte properties, coating characteristics, surface morphology, and corrosion behavior.

2. EXPERIMENTAL PROCEDURE AND DETAILS

2.1. Sample Preparation

The cast Mg AZ91D alloys were purchased and cut to 50 x 50 x 5 mm size using a wire-cut EDM. The composition of the purchased AZ91D is confirmed using EDX analysis, and it is Al 4.9 %, C 33.45 %, O 8.12 %, and Mg 53.44 %. The cut samples are pretreated to achieve proper bonding and to remove the greases and impurities. The substrates are first washed with acetone, then dipped in ethanol for 2 minutes, and then acid prickled for 3 minutes in a 10 %v sulphuric acid solution. At the end of each pretreatments process, the substrate is washed with distilled water to avoid the solution's contamination. After pretreatment of the substrates, it is immersed as quickly as possible into the prepared electrolyte solution. The proportion of the chemical used to prepare an electrolyte bath of 200 ml is given in table 1.

Table 1. Composition of bath for the electroless coating process

Description	**Quantity / Module**
Nickel Chloride	30 g/l
Sodium hypophosphite	40 g/l
Trisodium citrate	20g/l
Ammonium sulfate	80 g/l
Temperature	85ºC (±2ºC)
pH	9
Nano ZnO_2	1.5 g/l
Zwitterionic Surfactant [(N-dodecyl betaine)/(NDB)]	0.2g/l, 0.4 g/l, 0.6g/l& 0.8 g/l

2.2. Operating condition

The electrolyte bath contains nickel chloride as the metal source, Sodium hypophosphite as a reducing agent, trisodium citrate as a buffering agent, and the bath pH is regulated by ammonium sulfate. Further, the Surfactant NDB is added in various proportions such as 0.2, 0.4, 0.6, and 0.8 g/l to improve the electrolyte's surface tension in the CMC (critical micelle cell) to give more amount of active electrons on to the coated substrate.

2.3. Evaluate coating thickness

The weight gain analysis calculates the coating thickness, and the values are cross-checked with the aid of the scanning electron microscope using the metallographic section method. The high-precision digital weighing system has the least count of 0.0001g. The coated substrates are dried and weighed before four consecutive stable readings are obtained. The coating thickness is calculated using the equation 1 and equation 2.

$$\text{Coating Thickness (T)} = \text{Deposition rate (R)} \times \text{Deposition time } (t_t) \qquad \text{Eq. 1}$$

$$\mathrm{R}\ (\mu\mathrm{m/h}) = \frac{w_1 - w_2 \times 10^4}{d \times A \times t} \qquad \text{Eq. 2}$$

Where,

W_2 – Weight of substrate after coating, grams.
W_1 – Initial weight of the substrate before coating in grams.
d – Density of the deposit in g/cm^3.
A – Area of the substrate in cm^2.
t – Time duration of the substrate immersed in the electrolyte in hours (h).

2.4. Deposition Characterization

The electroless coated samples' surface morphology is analyzed using a high-resolution scanning electron microscope (HR-SEM) fitted with an energy-dispersive X-ray spectrometer (EDX) chemical composition of the coatings. The X-ray diffraction analysis was used to characterize the composite coating samples by the Bruker D_2 phaser power X-ray diffract meter using a CU X-ray tube with a step scan speed of 0.02/sec. From the obtained data differentiate, the phase values are identified. The roughness was measured using a benchmark instrument stylus tool to estimate the surface roughness (Ra). The measurement is repeated five times, and the average of five surface roughness values was considered. The microhardness test was identified using Vickers hardness tester, and the average was taken as per the ASTM E384 standard, and the test is conducted at a load of 200 gm for 15 sec. The Vickers hardness number (VHN) is calculated using equation 3.

$$VHN = \frac{2P \sin\frac{\theta}{2}}{{d_h}^2} \qquad \text{Eq. 3}$$

Where,

$\theta = 136^{\circ}$
d_h– Average length of diagonals

P- Applied load in kg.

Neutral salt spray tests are conducted to identify the corrosion resistance of the coated and uncoated samples. The coated samples are placed in the salt spray chamber for the evaluation of corrosion resistance. Two different 3.5 % NaCl solution was prepared with and without surfactant and sprayed over the coated samples at an expose angle of 30^o to 45^o from horizontal for a maximum time of 620 h. Before being loaded into the salt spray chamber, the samples are cleaned with acetone and rinsed with distilled water. The samples are thoroughly cleaned with acetone and rinsed with distilled water. The time required for rust to appear on the deposited surface was accurately recorded to assess each sample's corrosion rate. The weight-loss method's corrosion rate is expressed in mm/year (mmpy). The rate of corrosion is calculated by using a given equation 4.

$$CR = \frac{87.6 \times W}{\rho AT} \qquad \text{Eq. 4}$$

Where, W- weight loss (mg).

ρ – Material density (g/cm^3).

A – Area of the sample (cm^2).

T- Exposure time (h).

3. RESULTS AND DISCUSSIONS

3.1. Evaluate the coating thickness of substrate without and with surfactants

The deposition of the dispersed nickel particles over the surface is essential to improve the coated substrate's characteristics. In the initial coating condition (without surfactants), only a part of dispersed nickel is deposited, and the remaining floats on the surface of the electrolyte and coated on the surface of the beaker [25], shown in figure 1. The addition of the Zwitterionic Surfactant NDB in the electrolyte has improved the nickel composite particles' deposition. The Surfactant proportion is varied from 0.2 to 0.8 g/l increase in steps 0.2 g/l. It is seen that the increase in the proportion of NDB has improved the deposition rate and coating thickness attributed to the improved dispersion of the nanoparticles in the bath by NDB. Among the various ratios,0.6 g/l of NDB has a maximum coating thickness of 61µm as shown in figure 2. Further, increasing the surfactant in the electrolyte partially reduced the deposition rate and affects the coating thickness due to more amount of potential energy supply in the anodic reaction side, creating high electrostatic repulsive force.

Figure 1. Nickel composite metallic particles floated on the electrolyte

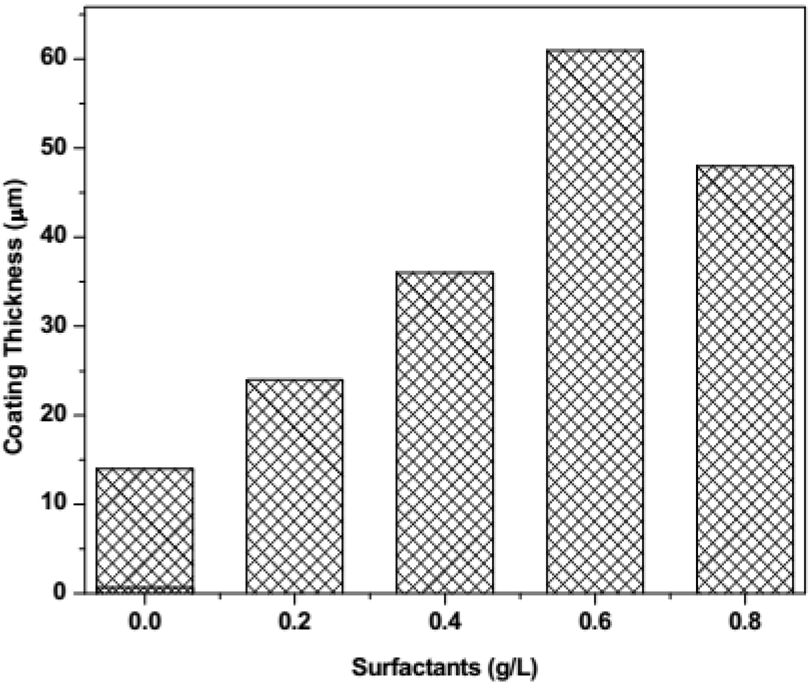

Figure 2. Coating thickness with and without Surfactant

3.2. Quality analysis of the deposits

The SEM micrographs of electroless Ni-P coatings and Ni-P nano ZnO_2 coating are shown in figures 3(a) and (b), respectively. The Ni-P surface shows a dense and mild white fungus-like formation, and without any surface, the damage is observed in figure 3 (a). In figure 3(b) Ni-P nano ZnO_2 coating without surfactants, fine nodular structures of nickel with black microvoids were observed due to uncontrolled zinc oxide reaction in the electrolyte. The embedded ZnO_2 particles in the Ni-P layer impact the surface, significantly expanding the boundary between nickel and the ZnO_2 particles introduced in the coating matrix [12].

Figure 3 (c, d, e & f) shows the surface morphology of Ni-P-nano-ZnO_2 coatings with different concentrations of Zwitterionic NDB Surfactants. The addition of zwitterion disperses ZnO_2 particles in the Ni-P matrix, it is seen that the uniformity of the dispersion increase with the increase in the volume of NDB. It is also seen that dispersion uniformity increase up to 0.6 g/l of NDB, and a further increase in volume reduced the dispersion of nanoparticles due to the creation of uncontrolled repulsive forces by excess volume of surfactants. In figure 3 (c), a nodular structure with microvoids was observed due to lower surfactant concentration. When the surfactant concentration is maintained below the CMC, the surface is formed smoothly and reduced micropores as shown in figure 3 (d-e), which is confirmed by the roughness test [33]. At a surfactant concentration is 0.8 g/l figure 3 (f), the micropores were formed due to high repulsive force by adding more surfactant are present in the electrolyte bath.

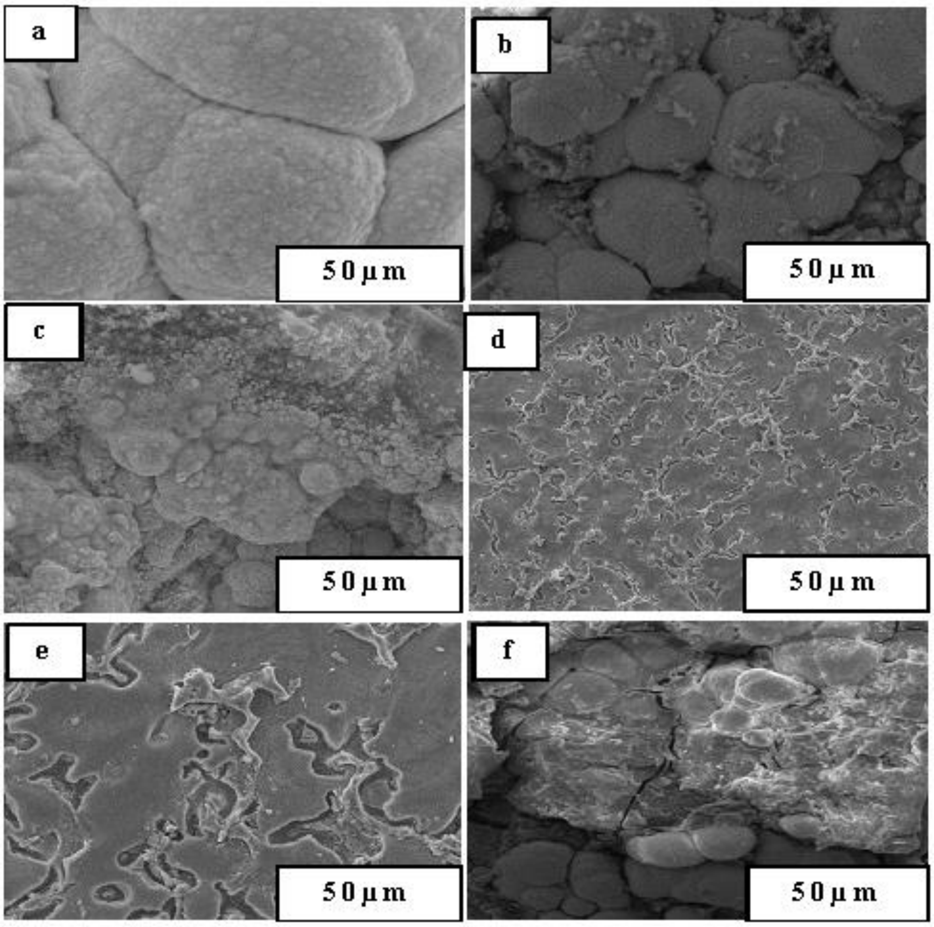

Figure 3. SEM image for (a) Ni-P coating without surfactant, (b) Ni-P-nano ZnO_2 coating without surfactant, with NDB surfactants (c) Ni-P-nano ZnO_2 coating with 0.2 g/l NDB surfactants (d) Ni-P-nano ZnO_2 coating with 0.4 g/l NDB surfactants (e) Ni-P-nano ZnO_2 coating with 0.6 g/l NDB surfactants (f) Ni-P-nano ZnO_2 coating with 0.8 g/l NDB surfactants

Figure 4 (a) to (e) show the diffraction patterns of full width at half maximum (FWHM) of diffraction peaks of electroless Ni-P nano-ZnO_2 composite coating without surfactants and with surfactant. In the coating deposit, there is a combination of amorphous and crystalline phases available. In all coatings, there is a single broad peak of $2\theta = 45°$, implying that the Ni-P deposit is amorphous. The crystalline ZnO_2 particles embedded in the Ni-P matrix were confirmed by the small peak of ZnO_2 particles near $2\theta = 37°$. The same has been confirmed by the EDX analysis shown in figure 5. The presence of ZnO_2 has increased from 0.8 wt% to 5.6 wt% with an increase in NDB volume by modifying the crystalline structure and improving the substrate's mechanical properties. However, when increasing the surfactant concentration crosses an optimal level at 0.6 NDB, the nanoparticle's wt% dramatically decreases, shown in table 2. This decrease in ZnO_2 affects the amorphous structure and forms an irregular nodular structure on the substrate's surface. A higher amount of surfactant is involved in the electrolyte that creates a higher repulsive force, affecting the deposit [17].

Table 2. Elemental composition of Ni-P Nano ZnO_2 composite coating

Deposited elemental wt (%)	**NDB Surfactant concentration (g/l)**				
	0	**0.2**	**0.4**	**0.6**	**0.8**
Ni K	92.8±1.2	90.7±1.2	86.9±0.5	90.1±0.7	93.6±0.6
P K	5.9±0.6	6.3±0.3	6.0±0.2	6.9±0.3	6.0±0.4
Zn K	0.8±0.3	2.6±0.2	3.4±0.4	5.6±0.4	0.9±0.1
O K	0.4±0.1	0.3±0.1	0.3±0.2	0.5±0.1	0.2±0.2

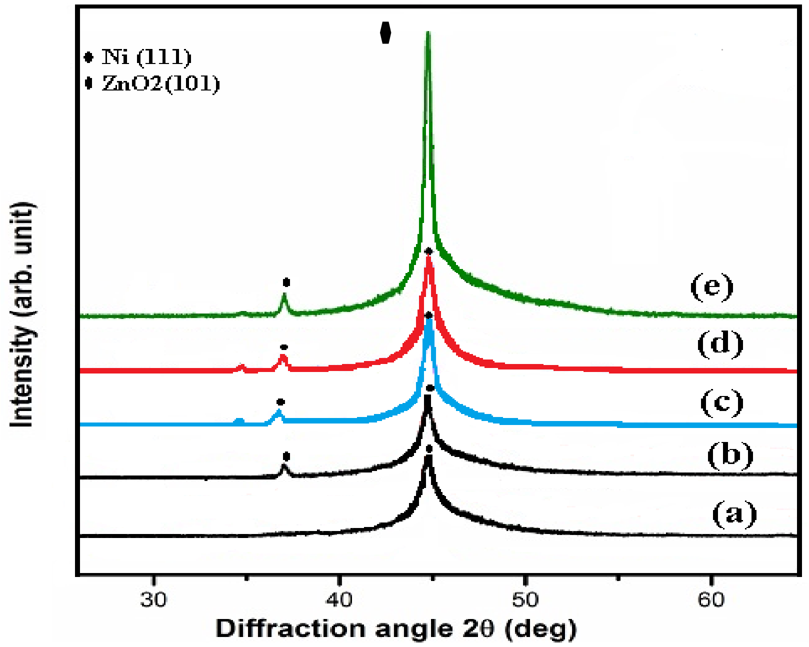

Figure 4. XRD image for (a) Ni-P without nano composite, (b) Ni-P-nano ZnO_2 without surfactant, with surfactant of (c) 0.2, (d) 0.4, (e) 0.6

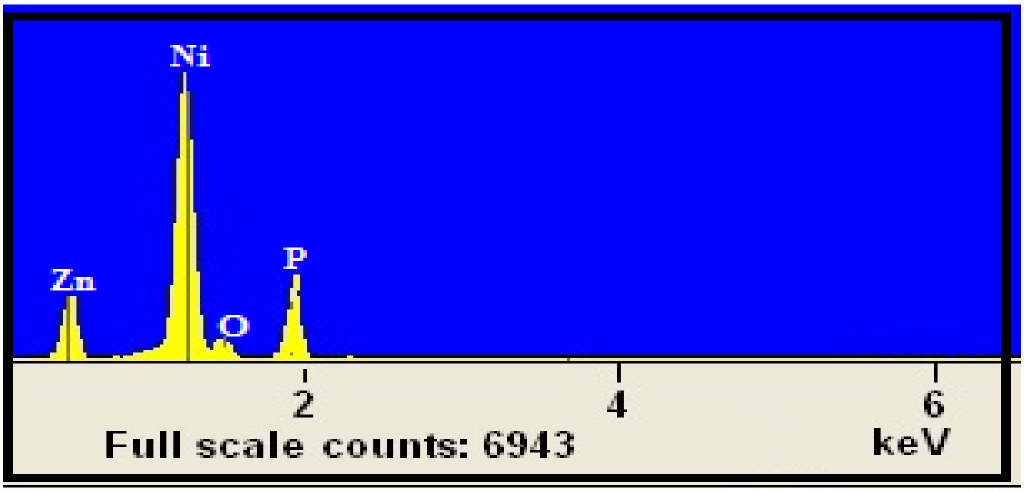

Figure 5. EDX image for Ni-P-nano ZnO_2 with Surfactant at 0.6 of NDB

3.3. Surface roughness

The surface roughness variation with the surfactant concentration is shown in Table 3. It is found that the Ra value of deposition was higher than the deposit with NDB surfactants regardless of their level of concentration. Also, it is noted that 0.6 NDB concentration has the least surface roughness; further increase in surfactant concentration harms the surface roughness value. This behavior is consistent with the other research outcomes on surface roughness of electroless plating reported [34]. The reduction of surface roughness at optimal concentration indicates the decrease of the particles' aggregation due to the even distribution of nanoparticles leads to a smoother surface [35].

Table 3. Average surface roughness of the coated sample

Roughness Measurements	**NDB Concentration (g/l)**				
	0	**0.2**	**0.4**	**0.6**	**0.8**
Ra (µm)	0.368	0.325	0.233	0.259	0.295

3.4. Hardness Measurement

The microhardness of electroless Ni-P-nano-ZnO_2 deposition with NDB surfactant and without surfactant is shown in figure 6. The nano ZnO_2 particles help to hinder the nickel matrix's plastic deformation, thus increasing the microhardness [5]. However, absence of surfactants, the agglomeration of ZnO_2 particles weakens the uniformity in the distribution of nanoparticles reduces hardness. The microhardness of Ni-P-nano-ZnO_2 deposits increases with Surfactant concentration and reaches the CMC and then drops. With the increase in surfactants concentration, the incorporation of particles into the matrix deposit has improved [30]. Moreover, when the Surfactant concentration reaches 0.6 g/l NDB, the amount of ZnO_2 dope is higher on the coated surface, so the mean microhardness value goes to a maximum of 720 HV100 at this concentration.

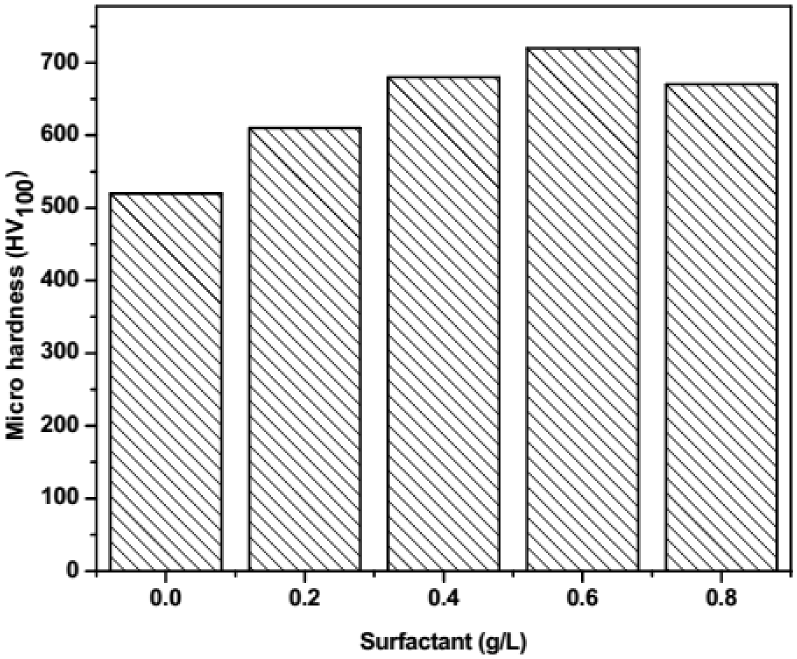

Figure 6. Microhardness measurements for with Surfactant (NDB) and without surfactant

3.5. Neutral salt spray test

A neutral salt spray test is an aggressive and effective way of testing the corrosion rate at composite coating substrates. In this experiment, all the coated samples were kept in the chamber for up to 620 h. Figure 7 shows the neutral salt spray examination to evaluate the corrosion with various surfactants used in the Ni-P –ZnO_2 composite coating. The plain composite layer has a high corrosion rate within 180 h, the first visible rust formation in the test sample due to the lack of nano ZnO_2 dispersed in the Ni-P matrix of the composite coating. Moreover, the corrosion resistance rate varies with the Surfactant of NDB with a reducing agent. The surfactant concentration of 0.6 NDB has withstood more than 580 h because of the fine elemental composition present in the composite coating. The higher amount of ZnO_2 particles deposit in the Ni-P metal matrix hinders the displacement of the particles of composite deposits and is attributable to corrosion resistance improvement [36]. Therefore, the NDB surfactant in Ni-P nano-ZnO_2 composite coating withstand more hours and found optimal corrosion resistance [37].

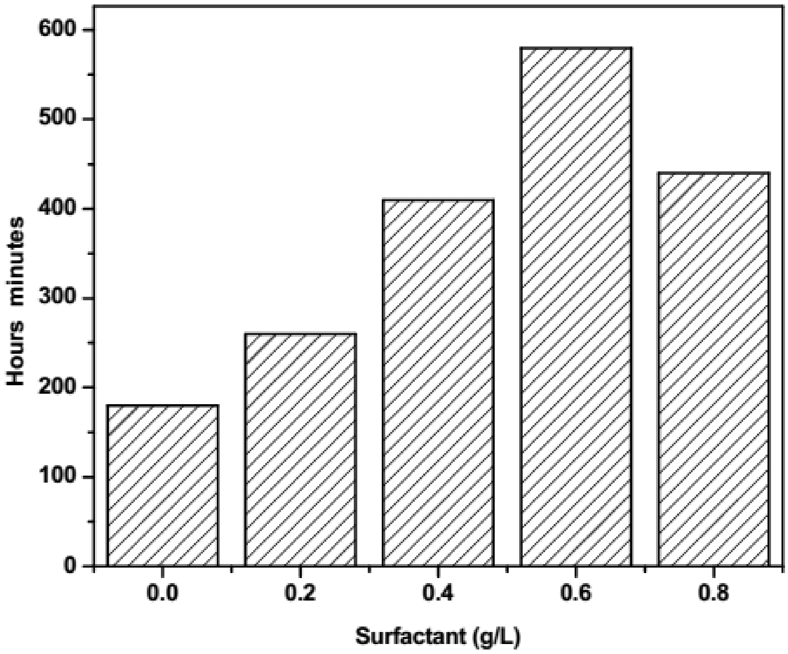

Figure 7. NSS test for analysis corrosion resistance of Ni-P nano ZnO_2 with different Surfactant (NDB) and without surfactants

4. CONCLUSIONS

The following conclusions have arrived based on the experimental investigation using NDB surfactant in the electroless NiP-nano-ZnO2 composite coating on magnesium alloy AZ91D substrate.

- The addition of an optimum volume of NDB has improved ZnO_2 in the coating because of the low surface tension electrolyte solution, results in uniform distribution of Nano ZnO_2 particle on the AZ91D.
- The Ni-P ZnO_2 composite coating's surface morphology shows an even distribution of ZnO_2 at 0.6 g/l of NDB Surfactant.
- The 0.6 g/l of NDB surfactant has produced the least surface roughness, and a further increase in Surfactant concentration has elevated the surface roughness value.
- The coating microhardness was improved significantly by NDB, and the maximum microhardness is 720 HV100 for 0.6 g/l NDB.

References

1. A. Shahriari, H. Aghajani, M.G. Hosseini, *Prog. Color. Color. Coatings,* 9 (2016) 151–162.
2. J. Sudagar, J.S. Lian, Q. Jiang, Z.H. Jiang, G.Y. Li, R. Elansezhian, *Prog. Org. Coatings*, 74 (2012) 788–793.
3. S. Ranganatha, T. V. Venkatesha, K. Vathsala, *Appl. Surf. Sci.*, 256 (2010) 7377–7383.
4. A. Yli-Pentti, Electroplating and Electroless Plating, Elsevier, (2014).
5. E. Georgiza, J. Novakovic, P. Vassiliou, *Surf. Coatings Technol.*, 232 (2013) 432–439.

6. V. Vitry, L. Bonin, *Surf. Coatings Technol.*, 311 (2017) 164–171.
7. T.J. Chen, Y. Ma, B. Li, Y.D. Li, Y. Hao, *Mater. Sci. Eng. A*, 445–446 (2007) 477–485.
8. Y. Li, K. Zhang, M. Zhang, Y. Zhang, T. Wu, H. Zhao, J. Su, Z. Wang, J. Wang, *J. Nanomater.*, 2020 (2020).
9. S. Nezamdoust, D. Seifzadeh, A. Habibi-Yangjen, *Trans. Nonferrous Met. Soc. China (English Ed.*, 30 (2020) 1535–1549.
10. S. Afroukhteh, C. Dehghanian, M. Emamy, *Prog. Nat. Sci. Mater. Int.*, 22 (2012) 318–325.
11. L. Bonin, V. Vitry, *Surf. Coatings Technol.*, 307 (2016) 957–962.
12. M.I. Ansari, D.G. Thakur, *Surfaces and Interfaces*, 7 (2017) 20–28.
13. S. Afroukhteh, C. Dehghanian, M. Emamy, *Prog. Nat. Sci. Mater. Int.*, 22 (2012) 480–487.
14. B.H. Chen, L. Hong, Y. Ma, T.M. Ko, *Ind. Eng. Chem. Res.*, 41 (2002) 2668–2678.
15. B. Simončič, V. Rozman, *Colloids Surfaces A Physicochem. Eng. Asp.*, 292 (2007) 236–245.
16. N. Nwosu, A. Davidson, C. Hindle, M. Barker, *Ind. Eng. Chem. Res.*, 51 (2012) 5635–5644.
17. D. Liu, Y. Yan, K. Lee, J. Yu, *Mater. Corros.*, 60 (2009) 690–694.
18. A. Zarebidaki, S.R. Allahkaram, *J. Alloys Compd.*, 509 (2011) 1836–1840.
19. N.S. Mohd Ali, A.R. Hassan, *Malaysian J. Anal. Sci.*, 20 (2016) 510–516.
20. R. Elansezhian, B. Ramamoorthy, P. Kesavan Nair, *Surf. Coatings Technol.*, 203 (2008) 709–712.
21. M.I. Ansari, D.G. Thakur, *Int. J. Technol. Res. Eng.*, 2 (2015) 1120–1124.
22. R. Zhang, P. Somasundaran, *Adv. Colloid Interface Sci.*, 123–126 (2006) 213–229.
23. A.M. Alsari, K.C. Khulbe, T. Matsuura, *J. Memb. Sci.*, 188 (2001) 279–293.
24. A.M. Khan, S.S. Shah, *J. Chem. Soc. Pakistan*, 30 (2008) 186–191.
25. R. Muraliraja, R. Elansezhian, J. Sudagar, A. V. Raviprakash, *J. Surfactants Deterg.*, 19 (2016) 1081–1088.
26. H.A. Ramezani-Varzaneh, S.R. Allahkaram, R. Faezi-Alivand, *Mater. Res. Express*, 6 (2019).
27. P. Makkar, D.D. Mishra, R.C. Agarwala, V. Agarwala, *Ceram. Int.*, 40 (2014) 12013–12021.
28. A.A. Zuleta, E. Correa, J.G. Castaño, F. Echeverría, A. Baron-Wiecheć, P. Skeldon, G.E. Thompson, *Surf. Coatings Technol.*, 321 (2017) 309–320.
29. M. Chorro, N. Kamenka, B. Faucompre, S. Partyka, M. Lindheimer, R. Zana, *Colloids Surfaces A Physicochem. Eng. Asp.*, 110 (1996) 249–261.
30. T.R. Tamilarasan, R. Rajendran, M. Siva, U. Sanjith, G. Rajagopal, J. Sudagar, *Wear*, 346–347 (2016) 148–157.
31. A. Sadeghzadeh-Attar, G. AyubiKia, M. Ehteshamzadeh, *Surf. Coatings Technol.*, 307 (2016) 837–848.
32. H. Wu, F. Liu, W. Gong, F. Ye, L. Hao, J. Jiang, S. Han, *Surf. Coat. Technol.*, 272 (2015) 25–32.
33. M.I. Ansari, S. Julka, D.G. Thakur, *J. Mol. Liq.*, 247 (2017) 22–33.
34. M. Momenzadeh, S. Sanjabi, *Mater. Corros.*, 63 (2012) 614–619.
35. M.I. Ansari, D.G. Thakur, *Surfaces and Interfaces*, 7 (2017) 20–28.
36. Y. hua SUN, R. chu WANG, C. qun PENG, Y. FENG, M. YANG, *Trans. Nonferrous Met. Soc. China (English Ed.*, 27 (2017) 1455–1475.
37. X.B. Chen, M.A. Easton, N. Birbilis, H.Y. Yang, T.B. Abbott, Corrosion-Resistant Electrochemical Plating of Magnesium (Mg) Alloys, Woodhead Publishing Limited, (2013).